

Cite this: *Chem. Commun.*, 2019, 55, 13275Received 8th July 2019,  
Accepted 9th October 2019

DOI: 10.1039/c9cc05231c

rsc.li/chemcomm

**Magnetic affinity beads functionalized with lactose and ruthenium/dcbpy complexes were developed. Using MAUra, a catalyst-proximity labelling reagent, the catalytic labeling of lactose-binding proteins was achieved with high selectivity on the beads. The first unbiased identification of cellular endogenous lectins bound to lactose (galectin-1 and galectin-3) was achieved with chemical labelling on the affinity beads.**

Techniques for identifying proteins bound to ligands are important for elucidating the mechanisms underlying biological pathways and identifying the interactions between proteins and ligands. Most of the studies on protein–ligand interactions focus on high affinity interactions ( $K_D < 10^{-6}$  M). Because many conventional approaches fail to apply weak interactions ( $K_D > 10^{-4}$  M), information about weak protein–ligand complexes is still scarce. Weak and transient protein–protein interactions ( $K_D > 10^{-4}$  M),<sup>1,2</sup> such as lectin–carbohydrate interactions ( $K_D = \sim 10^{-3}$  M), are exploited for cell differentiation, adhesion, and rapid turnover cell signaling, and are one of the key factors to understating rapid responses of cellular systems.<sup>3</sup> Although NMR, isothermal titration calorimetry (ITC) and surface plasmon resonance (SPR) have been applied to analyze such weakly bound proteins, these methods require purified target proteins. Therefore it is difficult to utilize them for the identification of an unknown protein binding to a ligand,<sup>4</sup> and thus, development of technology for the detection/identification of weak protein–ligand interactions is still an urgent requirement in molecular biology.

## Catalyst-proximity protein chemical labelling on affinity beads targeting endogenous lectins†

 Michihiko Tsushima,<sup>ab</sup> Shinichi Sato,<sup>id</sup>\*<sup>a</sup> Tatsuya Niwa,<sup>c</sup> Hideki Taguchi<sup>c</sup> and Hiroyuki Nakamura<sup>id</sup>\*<sup>a</sup>

Selective chemical labelling of ligand-binding proteins with covalent bond formation enables the detection of proteins weakly bound to ligands, and photoaffinity probes have been developed and widely used for detecting target proteins with weak affinity.<sup>5,6</sup> In the case of lectins, the affinity can be increased by using carbohydrate dendrimers due to the multivalent binding effect between lectin oligomers and carbohydrates.<sup>7</sup> Utilizing this property, multivalent carbohydrate photoaffinity probes were developed (Fig. 1a).<sup>8–13</sup> For example, Pieters and co-workers achieved the labelling of targets that were added in a sufficient amount into cell lysate using multivalent carbohydrate photoaffinity probes.<sup>14</sup> However, the applications of these methods are limited to purified lectin or protein mixture systems containing artificially added lectins, and the selectivity to lectins is not sufficient. In fact, labelling of cellular endogenous lectins has not been reported so far. This limitation is generally caused by the low efficiency of the photoaffinity crosslinking reaction

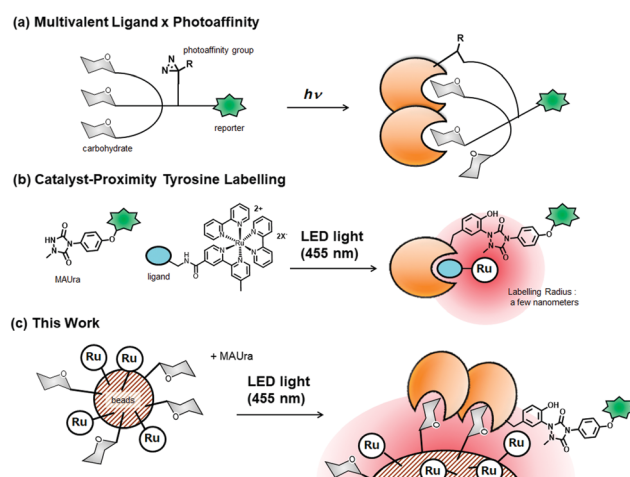


**Fig. 1** Concept of this work. (a) Photoaffinity probe containing multivalent carbohydrate ligands. (b) Catalyst-proximity tyrosine residue labelling using a ligand-conjugated Ru(bpy)<sub>3</sub> photocatalyst. (c) This work: lectin labelling on catalyst-functionalized affinity beads.

<sup>a</sup> Laboratory for Chemistry and Life Science, Institute of Innovative Research, Tokyo Institute of Technology, 4259-R1-13, Nagatsuta-cho, Midori-ku, Yokohama, Kanagawa 226-8503, Japan. E-mail: shinichi.sato@res.titech.ac.jp, hiro@res.titech.ac.jp

<sup>b</sup> School of Life Science and Engineering, Tokyo Institute of Technology, Japan

<sup>c</sup> Cell Biology Center, Institute of Innovative Research, Tokyo Institute of Technology, 4259-S2-19, Nagatsuta-cho, Midori-ku, Yokohama, Kanagawa 226-8503, Japan

† Electronic supplementary information (ESI) available. See DOI: 10.1039/c9cc05231c

(less than 10%).<sup>15,16</sup> On the other hand, we developed a catalytic tyrosine residue labelling technique that uses Ru(bpy)<sub>3</sub><sup>2+</sup> as the photocatalyst.<sup>17,18</sup> In this method, a tyrosine residue is oxidized by single-electron transfer (SET) of a ruthenium photocatalyst and a tyrosyl radical is generated to react with a labelling reagent. Using a ligand-conjugated catalyst, target protein selective labelling was achieved due to the proximity property of the SET reaction (Fig. 1b). Recently, we discovered that 1-methyl-4-arylurazole (MAUra) efficiently labels tyrosine located a few nanometers from Ru(bpy)<sub>3</sub><sup>2+</sup>.<sup>19</sup> We also performed target protein purification and labelling simultaneously using Ru-photocatalyst-functionalized beads.<sup>20</sup> We thought that MAUra could selectively label bead-binding proteins located in close proximity to the photocatalyst functionalized on the beads. Using this system, weak and transient ligand binding proteins, which cannot be pulled down by conventional affinity chromatography, can be labelled on the beads. In this communication, we achieved the first chemical labelling and highly sensitive detection of endogenous carbohydrate-binding proteins through proximity-dependent labelling using MAUra on ruthenium/dcbpy complex functionalized beads (Fig. 1c).

To demonstrate the concept, we chose peanut agglutinin (PNA,  $K_D = 770 \mu\text{M}^{21}$  for lactose), a lectin that is derived from *Arachis hypogaea* fruit and recognizes the  $\beta(1-4)$ -galactoside group, and  $\beta$ -D-lactose as the model target protein and ligand, respectively. Sakurai and co-workers reported that the binding affinity between PNA and  $\beta$ -D-lactose was drastically increased by the immobilization of  $\beta$ -D-lactose on nanoparticles.<sup>12</sup> We synthesized beads **1** and **2**, on which the Ru(bpy)<sub>3</sub> complex (bead **1**) and Ru/dcbpy complex (bead **2**) were immobilized, respectively, with  $\beta$ -D-lactose (see the ESI,† Section S2–S9, for details on bead preparation). In order to evaluate the labelling efficiency and the PNA selectivity for each catalyst or the reaction field on beads, PNA labelling with MAUra-azide (**3**) was performed in PNA-containing HeLa cell lysate using bead **1**, bead **2**, or lactose-conjugated Ru photocatalyst **4**. When **4** was used as the catalyst, much lactose-independent labelling was observed (lane 3, Fig. 2b). This may be due to the weak affinity of the ligand and the fact that most of the ligand-conjugated catalysts did not bind to PNA selectively. Improved labelling selectivity was observed in the case of bead **1** (lane 5, Fig. 2b). We have reported that nonspecific protein binding on beads is suppressed by changing the catalyst from the Ru(bpy)<sub>3</sub> to Ru/dcbpy complex.<sup>20</sup> By using bead **2**, we succeeded in the selective labelling of PNA in the protein complex mixture (lane 7, Fig. 2b).<sup>22</sup> PNA labelling was hardly observed in the presence of an excess amount of  $\beta$ -D-lactose, suggesting that the PNA-selective labelling was lactose-dependent (lane 8, Fig. 2b and Fig. S2, ESI†). Under the conditions where other labelling reagents were used instead of **3**, both the labelling efficiency and selectivity were insufficient (Fig. S3, ESI†). These results suggest that the labelling radius of the radical species of MAUra is suitable for proximity labelling of bead-binding proteins on bead **2**. Not only when targeting PNA but also in model experiments targeting carbonic anhydrase, the ligand- and Ru/dcbpy-complex-functionalized beads labelled target proteins in protein

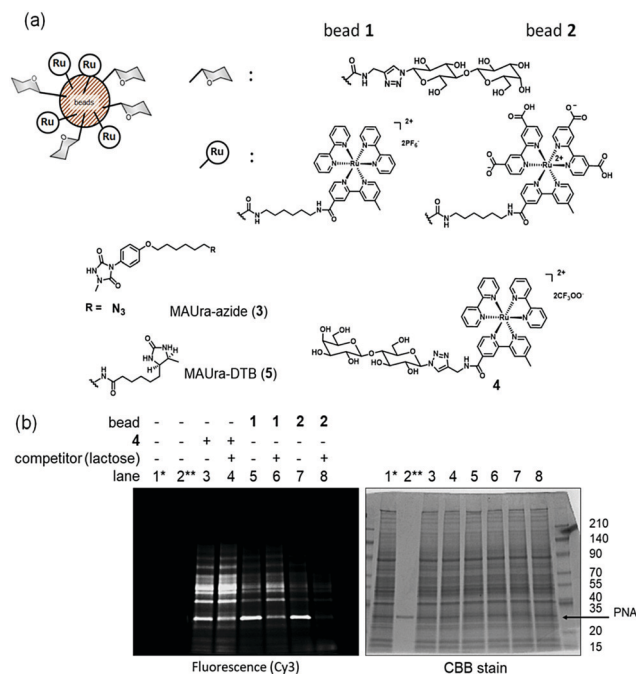


**Fig. 2** PNA-selective labelling in PNA-containing HeLa cell lysate using a lactose-conjugated photocatalyst or photocatalyst-functionalized affinity beads. (a) Structures of the ligand, photocatalyst, and labelling reagents. (b) PNA-selective labelling using bead **1**, bead **2** or lactose-conjugated Ru photocatalyst **4**. A mixture of PNA (1  $\mu\text{M}$ ) and HeLa cell lysate (1.0 mg mL<sup>-1</sup> protein) in lysis buffer (pH 7.4) was photo-irradiated (455 nm LED) in the presence of **3** (500  $\mu\text{M}$ ) at 0 °C for 5 min. Azide-labelled proteins were visualized by a copper-free click reaction with DBCO-Cy3. \*Input: PNA (1  $\mu\text{M}$ ) containing HeLa cell lysate (1.0 mg mL<sup>-1</sup> protein). \*\*PNA control (1  $\mu\text{M}$ ).

mixtures more selectively than the ligand-conjugated Ru(bpy)<sub>3</sub> complex (Fig. S4, ESI†).

As another type of labelling reagent, we previously reported desthiobiotin-conjugated MAUra (MAUra-DTB, **5**, Fig. 2a).<sup>19</sup> Using the binding property of desthiobiotin to streptavidin, labelled proteins can be enriched with streptavidin beads. Adopting the enrichment system, we evaluated the labelling efficiency of PNA on bead **2**. PNA was labelled by **5** and the enriched proteins were quantified by SDS-PAGE and silver staining, compared with PNA of known concentrations. As a result, 22% labelling efficiency was achieved (Fig. S5, ESI†). This value is higher than the general efficiencies of conventional photoaffinity labelling methods targeting lectins (less than 10%).<sup>15,16</sup> In addition, in order to identify the labelled site, PNA was labelled with MAUra-N<sub>3</sub> (**3**), and the labelled PNA was reacted with DBCO-Cy3, in-gel tryptic-digested, and analyzed by LC-MS. In a control experiment using Ru(bpy)<sub>3</sub>Cl<sub>2</sub>, many peaks were visible on the fluorescence spectrum because of the random site tyrosine labelling on PNA (Fig. S6d, ESI†). On the other hand, in the case of bead **2**, limited peaks were observed on the fluorescence spectrum, suggesting that the labelling proceeded site-selectively. We could identify the labelled peptide fragment by MS measurement of the labelled peak separated by HPLC. The identified peptide fragment contains

two tyrosines (Y124 and Y129) in its sequence (Fig. S6b and e, ESI†). Although we could not identify which tyrosine is labelled selectively by LC-MS/MS analysis, the topological positions of both Y124 and Y129 were in close proximity to the lactose binding site according to the X-ray structure of PNA (PDB: 2pel, Fig. S7, ESI†).<sup>23</sup> This result suggested that PNA bound to beads *via* lactose binding, and was selectively labelled with tyrosine residue(s) around the binding site. This result also suggested that catalyst-proximity labelling on the beads enabled site-selective labelling in the ligand binding site of target proteins as well as target protein selective labelling in the protein mixture.

Then, we performed labelling of an endogenous lactose-binding protein in A431 cell lysate using bead 2. The bead-binding protein was labelled by MAUra-DTB (5), and the labelled protein was enriched with streptavidin beads. The enriched protein was digested with trypsin and identified by LC-MS/MS. To distinguish lactose-independent labelling *via* non-specific bead binding, we performed a control experiment. In the presence of an excess amount of free lactose, only lactose-mediated binding on beads should be inhibited, resulting in the labelling inhibition of lactose-binding proteins (Fig. 3a). We obtained a list of enriched proteins in both experiments by LC-MS/MS analysis in the absence or presence of an excess amount of free lactose. From this list, we extracted proteins that were efficiently labelled in the absence of free lactose, and whose labelling was suppressed in the presence of free lactose (see the ESI,† Table S1, for details on extraction conditions). Fig. 3b shows the list of extracted proteins. In this list, we focused on galectin-1 and galectin-3 (shown in red), which are proteins that bind specifically to  $\beta$ -galactoside. The results were also confirmed by Western blot analysis of enriched proteins using anti-galectin-1 and anti-galectin-3 antibodies (Fig. S8, ESI†). The results are reasonable because lactose is a typical  $\beta$ -galactoside and

the binding between lactose and galectins is well studied. However, to our knowledge, this is the first report of lectin identification from the cellular protein mixture without any bias. Previous lectin-labelling studies were based on model experiments in which purified lectins or lectin-added protein mixtures are used. In this communication, the combination of the multivalent effect on the beads and the labelling of bead-binding proteins enabled us to identify the binding of cellular endogenous lectins and lactose. Furthermore, integrin, inactive tyrosine protein kinase, and heterogeneous nuclear ribonucleoprotein (hnRNP) were also detected by LC-MS/MS analysis (shown in blue in Fig. 3b and Fig. S9–11). It was reported that these proteins form protein complexes *via* interactions between galectin-3 and glycans on the protein surface.<sup>24–26</sup> Thus, this result suggests that not only proteins that bind to lactose but also protein–protein interaction partners were labelled on the beads. The binding affinity between lactose and galectin-1 or galectin-3 is weak ( $K_D$ : millimolar order).<sup>27,28</sup> According to a previously reported procedure,<sup>29</sup> we observed the inhibition of His-tagged galectin-3 binding to asialofetuin (ASF) on an ELISA plate on incubation with monomeric lactose or bead 2. In the case of monomeric lactose, the  $IC_{50}$  value was 3.87 mM. On the other hand, in the case of bead 2, the  $IC_{50}$  value was 0.398  $\mu$ M, suggesting that the binding affinity was improved by 10 000-fold by lactose functionalization on the beads (Fig. S12, ESI†). Although the binding affinity was improved by the multivalent binding effect on the beads, the purification by the conventional affinity purification method was unsuccessful because the binding affinity is not sufficient to pull down galectin-1 and -3 (Fig. S13, ESI†). These results indicate that the proximity labelling of bead-binding proteins is useful for detection and identification, and would be applicable to weak affinity targets that cannot be detected by the conventional affinity purification method.

We also applied this labelling method to two-dimensional fluorescence difference gel electrophoresis (2D-DIGE). Bead-binding proteins were labelled by MAUra-azide (3) and the azide-labelled proteins were visualized by copper-free click chemistry with dibenzocyclooctyne-conjugated Cy5 (DBCO-Cy5). To distinguish from lactose-independent labelling, we performed the same experiment in the presence of an excess amount of free lactose, and the labelled proteins were visualized by DBCO-Cy3. The Cy3- and Cy5-labelled samples were mixed, and the proteins were separated by two-dimensional electrophoresis (Fig. 4). The use of two fluorophores facilitated the distinction between lactose-dependent labelling and lactose-independent labelling. Galectin-1 and galectin-3 could be detected as spots that were selectively labelled with Cy5.

In conclusion, we have developed proximity-dependent labelling of affinity-bead-binding proteins. We labelled lectin in cell lysate using lactose- and ruthenium-photocatalyst-functionalized beads. We succeeded in the selective labelling of PNA in PNA-containing HeLa cell lysate using the beads. The labelling on the beads showed higher efficiency and selectivity than when using a lactose-conjugated ruthenium photocatalyst. We carried out the labelling of endogenous lactose-binding proteins in A431 cell lysate. The first unbiased labelling and

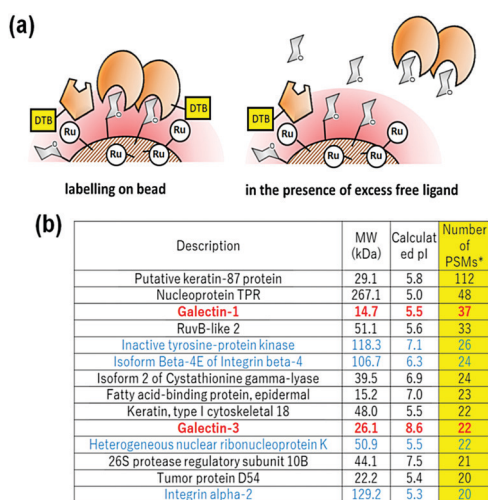


Fig. 3 Identification of a bead-binding protein by labelling with 5, desthiobiotin affinity enrichment, and LC-MS/MS detection. (a) Scheme of bead-binding protein labelling in the absence and presence of excess free ligand. Labelling was performed using beads 2 (5.0 mg mL<sup>-1</sup>) and 5 (500  $\mu$ M) in A431 cell lysate (3.0 mg mL<sup>-1</sup>). (b) Data-extracted list of labelled proteins in the absence of a free ligand. \*Peptide spectrum matches in LC-MS/MS of enriched proteins.

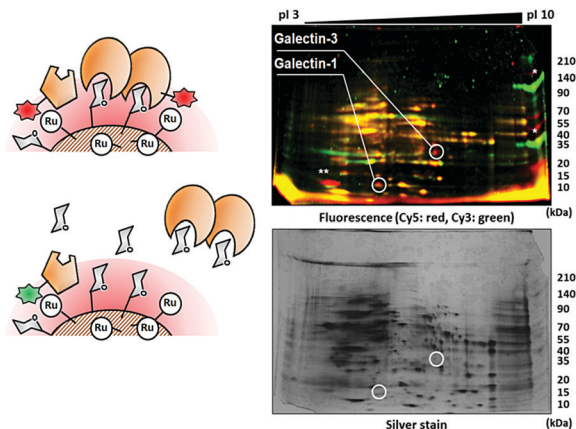


Fig. 4 2D-DIGE analysis of labelled proteins. After labelling with **3** (500  $\mu$ M), azide-labelled proteins were visualized by the copper-free click reaction with DBCO-Cy5 or DBCO-Cy3. Cy5-labelled proteins are shown in red and Cy3-labelled proteins are shown in green. Identified lactose-binding proteins (galectin-1 and galectin-3) by LC-MS/MS analysis as indicated by white circles. \*Green bands on the left are molecular weight markers (140 kDa and 35 kDa). \*\*A spot (MW  $\sim$  15 kDa, pI  $\sim$  4) labelled efficiently with Cy5 could not be identified by trypsin digestion and LC-MS/MS.

identification of cellular endogenous lectins were achieved. Endogenous galectin-1 and -3 ( $10^{-3}$  M  $K_D$  values with lactose) were labelled and identified as cellular endogenous lactose-binding proteins by LC-MS/MS and Western blot. Furthermore, the protein-protein interaction partners of galectin-3 were also labelled and identified. These results suggest that the proximity labelling of bead-binding proteins enables the detection of ligand-binding proteins with weak affinity. Not only the direct ligand-binding proteins, but also protein complex containing ligand-binding proteins could be labelled on the bead surface. This technique can be used to identify ligand-binding proteins that are difficult to analyze by other conventional affinity purification methods. Applications are not limited to the identification of carbohydrate-binding proteins. By changing the ligand part, various protein-ligand interactions can be identified. We are now in a position to identify ligand-binding proteins with weak affinity by this technique.

M. T. gratefully acknowledges the financial support from JSPS (ID No. 18J21621). This work was partially supported by Grants-in-Aid for “Grant-in-Aid for Young Scientists (A) (15H05490 to S. Sato)”, “Homeostatic regulation by various types of cell death (15H01372 to S. Sato)”, and “Chemistry for Multimolecular Crowding Biosystems (18H04542 to H. Nakamura)” from MEXT, Japan.

## Conflicts of interest

There are no conflicts to declare.

## Notes and references

- 1 J. R. Perkins, I. Diboun, B. H. Dessailly, J. G. Lees and C. Orengo, *Structure*, 2010, **18**, 1233–1243.
- 2 J. Yoo, T. S. Lee, B. Choi, M. J. Shon and T. Y. Yoon, *J. Am. Chem. Soc.*, 2016, **138**, 14238–14241.
- 3 J. Qin and A. M. Gronenborn, *FEBS J.*, 2014, **281**, 1948–1949.
- 4 A. D. Thompson, A. Dugan, J. E. Gestwicki and A. K. Mapp, *ACS Chem. Biol.*, 2012, **7**, 1311–1320.
- 5 (a) G. A. Korshunova, N. V. Sumbatyan, A. N. Topin and M. T. Mchedlidze, *Mol. Biol.*, 2000, **34**, 823–839; (b) F. Kotzyba-Hibert, I. Kapfer and M. Goeldner, *Angew. Chem., Int. Ed. Engl.*, 1995, **34**, 1296–1312; (c) G. Dormán, H. Nakamura, A. Pulsipher and G. D. Prestwich, *Chem. Rev.*, 2016, **116**, 15284–15398.
- 6 I. Hamachi, T. Nagase and S. Shinkai, *J. Am. Chem. Soc.*, 2000, **122**, 12065–12066.
- 7 S. Cecioni, A. Imberty and S. Vidal, *Chem. Rev.*, 2015, **115**, 525–561.
- 8 K. G. Rice, O. A. Weisz, T. Barthel, R. T. Lee and Y. C. Lee, *J. Biol. Chem.*, 1990, **265**, 18429–18434.
- 9 G. Lauc, R. T. Lee, J. Dumić and Y. C. Lee, *Glycobiology*, 2000, **10**, 357–364.
- 10 M. R. Lee, D. W. Jung, D. Williams and I. Shin, *Org. Lett.*, 2005, **7**, 5477–5480.
- 11 L. Ballell, M. Van Scherpenzeel, K. Buchalova, R. M. J. Liskamp and R. J. Pieters, *Org. Biomol. Chem.*, 2006, **4**, 4387–4394.
- 12 K. Sakurai, Y. Hatai and A. Okada, *Chem. Sci.*, 2016, **7**, 702–706.
- 13 A. Wibowo, E. C. Peters and L. C. Hsieh-Wilson, *J. Am. Chem. Soc.*, 2014, **136**, 9528–9531.
- 14 T. Rungrotmongkol, P. Yotmanee, N. Nunthaboot and S. Hannongbua, *Curr. Pharm. Des.*, 2011, **17**, 1720–1739.
- 15 M. Hashimoto and Y. Hatanaka, *Eur. J. Org. Chem.*, 2008, 2513–2523.
- 16 K. Sakurai, *Asian J. Org. Chem.*, 2015, **4**, 116–126.
- 17 S. Sato and H. Nakamura, *Angew. Chem., Int. Ed.*, 2013, **52**, 8681–8684.
- 18 S. Sato, K. Morita and H. Nakamura, *Bioconjugate Chem.*, 2015, **26**, 250–256.
- 19 S. Sato, K. Hatano, M. Tsushima and H. Nakamura, *Chem. Commun.*, 2018, **54**, 5871–5874.
- 20 M. Tsushima, S. Sato and H. Nakamura, *Chem. Commun.*, 2017, **53**, 4838–4841.
- 21 K. J. Neurohr, D. R. Bundle, N. M. Young and H. H. Mantsch, *Eur. J. Biochem.*, 1982, **310**, 305–310.
- 22 The amount of immobilized compound on the beads used in Fig. 1, lane 7 was lactose: 3.8 nmol  $\text{mg}^{-1}$  beads, Ru/dcbpy complex: 20.0 nmol  $\text{mg}^{-1}$  beads. See Fig. S1 (ESI $^\dagger$ ).
- 23 R. Banerjee, K. Das, R. Ravishankar, K. Suguna, A. Surolia and M. Vijayan, *J. Mol. Biol.*, 1996, **259**, 281–296.
- 24 E. H. Yang, J. Rode, M. A. Howlander, M. Eckermann, J. T. Santos, D. Hernandez Armada, R. Zheng, C. Zou and C. W. Cairo, *PLoS One*, 2017, **12**, 1–17.
- 25 S. Jaiswal and K. K. Srivastava, *Biochem. Biophys. Res. Commun.*, 2018, **498**, 884–890.
- 26 K. Fritsch, M. Mernberger, A. Nist, T. Stiewe, A. Brehm and R. Jacob, *BMC Cancer*, 2016, **16**, 1–10.
- 27 M. C. Miller, I. V. Nesmelova, D. Platt, A. Klyosov and K. H. Mayo, *Biochem. J.*, 2009, **421**, 211–221.
- 28 J. Seetharaman, A. Kfanigsberg, R. Slaaby, H. Leffler, S. H. Barondes and J. M. Rini, *J. Biol. Chem.*, 1998, **273**, 13047–13052.
- 29 D. Laaf, P. Bojarová, H. Pelantová, V. Křen and L. Elling, *Bioconjugate Chem.*, 2017, **28**, 2832–2840.